# Prediction of axle fatigue life based on field measurements

Michele MAGLIO[1], Elena KABO[1], Anders EKBERG[1], Pär SÖDERSTRÖM[2], Daniele REGAZZI[3], Steven CERVELLO[3]

[1]CHARMEC / Dept of Mechanics and Maritime Sciences, Chalmers University of Technology, Gothenburg, Sweden
[2]SJ AB, Stockholm, Sweden
[3]Lucchini RS, Lovere, Italy
Corresponding Author: Michele Maglio (michele.maglio@chalmers.se)

## Abstract

In order to facilitate the adoption of a condition-based maintenance approach for railway axles, more knowledge regarding the occurrence of operational axle stresses is needed. The current work aims at modelling the operational loading of wheelset axles by means of frequency distributions of stress amplitudes. The raw strain spectra have been gathered during field measurements using an instrumented telemetry mounted on a powered axle running within the Swedish railway network. Strain spectra are transformed into bending stress spectra which are used to estimate the statistical distributions of axle stresses for different track sections. Stress spectra obtained from field measurements as well as the statistical distributions representing these are used as input to fatigue life analyses. In these analyses, Wöhler (stress–cycles) curves obtained under different hypotheses are used to predict axle lives under varying operational conditions and for different properties of the axle material and surface. The method proposed in this paper allows to rapidly post-process data obtained during maintenance of the track and of the wheelset. This would help train operators to keep control on the status of their rolling stock assets, optimise maintenance and inspection intervals, and thereby save money and increase operational reliability.

**Keywords:** Field measurements, statistical analyses, stress spectra, railway wheelset fatigue life, rolling stock maintenance.

## 1. Introduction

Inspection intervals of railway axles and other components of the running gear are usually scheduled depending on the distance that the vehicle has travelled. This approach in scheduling maintenance, however, does not account for the current health status of the railway wheelset nor for the operational conditions to which the wheelset has been subjected. As a result, some trains are put out of service even though their running gear is not in need for maintenance. Other trains which have been subjected to more significant loads might instead be maintained too late. This can result in higher maintenance costs, in potential safety issues as well as in lower fleet availability.

To avoid these downsides, train operators are currently aiming at optimising their maintenance intervals by prolonging them as long as the parameters used to monitor a certain asset fall in a “safe” range. Such an approach, named condition-based maintenance, requires more knowledge regarding the occurrence of axle stress amplitudes, as high stress amplitude values can have a negative influence on the wheelset fatigue life.

Axle stress frequency distributions (spectra) have been investigated in previous studies. In Ref. [1], for example, operational loadings of wheelset axles have been represented by summing up contributions from trains running over straight tracks, curved tracks and switches and crossings. In Ref. [2], bending stress spectra have been obtained from field tests and numerical simulations. The increase in axle stress magnitudes due to increasing levels of wheel out-of-roundness (OOR) and rail roughness has been assessed. The residual lifetime of axles characterised by the presence of cracks was estimated in Ref. [3], where a measured load spectrum was obtained by dividing measured bending amplitudes in blocks depending on the ratio between static and measured axle loads. In the present investigation, which is based on the studies performed in Ref. [4], stress spectra are differentiated depending on the specific section of the railway network where the train is travelling. The numbers of narrow curves, switches and crossings present in different track sections has an influence on the stress spectra.

The data used in this work have been gathered in Ref. [2] in terms of bending strains using an instrumented telemetry system installed on a powered wheelset located at one end of a regional train. Axle bending strain spectra measured on different track sections have been used to estimate statistical distributions of axle stresses which have later been used as input to fatigue life analyses

The obtained statistical distributions of stresses can be used to predict the axle fatigue life accounting for the influence of variations in axle surface conditions. Fatigue analyses may help in identifying permissible levels in axle stresses at which precautions need to be taken to avoid failures for determined axle surface conditions. This would allow train operators to adopt a predictive maintenance approach and to prioritise wheelsets where the estimated residual fatigue lifetime is more critical.

## 2. The field test

### 2.1 The telemetry system

An instrumented telemetry system named SmartSet®, developed by Lucchini RS, has been installed on a powered axle mounted under one end of a regional train in Sweden, see Ref. [2]. The telemetry system consists of a data acquisition computer, a telemetry module and strain gauges placed on the axle at a distance of 80 mm from the wheel seat, where stress concentration effects can be neglected. The axle load acting on the instrumented wheelset is around 18.25 tonnes. Signals from the strain gauges are processed using a rainflow count algorithm and stored in cumulative matrices of strain mean values and amplitudes. Matrices are sent to a remote server when the train is at specific GPS locations, thus allowing to relate measured spectra to specific sections of the network. More information on the telemetry system can be found in Ref. [2].

### 2.2 Axle stress spectra

In this work, stress spectra have been post-processed and plotted by dividing the number of cycles falling within a stress amplitude bin with the total number of stress cycles measured during a given train ride. This allows for an easier comparison of spectra obtained for stretches of different lengths. In addition, the work presented in this paper is based on measurements obtained when the instrumented wheelset is in the leading position. Indeed, the first wheelset in the train suffers from higher wheel–rail contact forces and the resulting higher stresses can lead to a significant shortening of the fatigue life.

To account for the effect of mean stresses, equivalent amplitudes $\sigma_{ar}$ computed according to the Smith-Watson-Topper (SWT) criterion are used in our analyses

$$\sigma_{ar} = \sqrt{\sigma_{max}\sigma_a} \qquad (\sigma_{max} > 0) \tag{1}$$

where $\sigma_{max}$ and $\sigma_a$ are respectively the maximum stress value in a cycle, see Ref. [5]. More information on the way stress spectra are post-processed can be found in Refs. [2] and [4].

### 2.3 Statistical interpretation of stress spectra

Fig.1 shows stress spectra obtained between May 2019 and November 2020 for two different stretches (Gothenburg–Skövde and Skövde–Hallsberg) which are part of a mixed traffic railway line connecting Gothenburg and Stockholm. These track sections are expected to have similar levels of rail roughness. It can be noticed that, for both stretches, most of the measured equivalent stress amplitudes fall between 35 MPa and 40 MPa. This is expectable as most of the equivalent stress amplitudes are only influenced by the static load

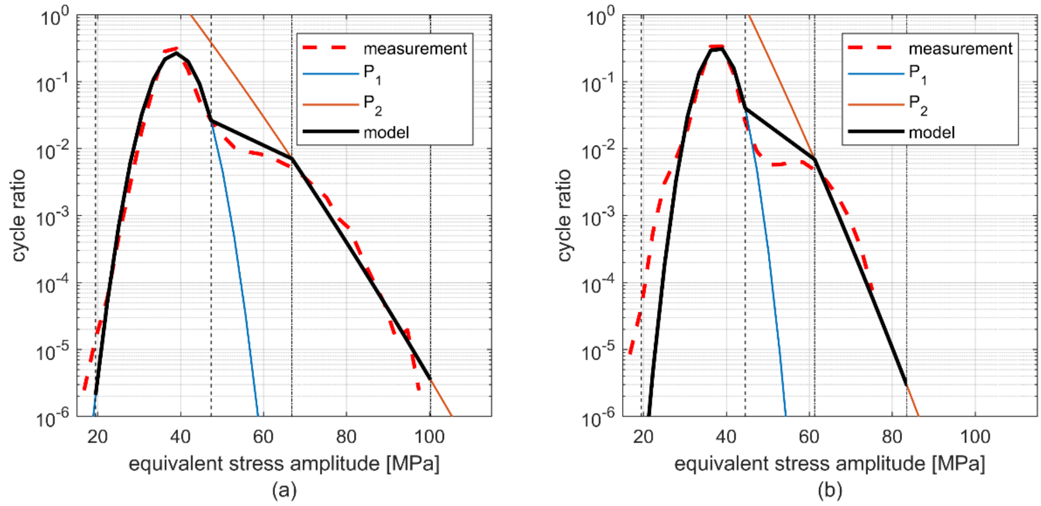


**Figure 1:** Stress spectra showing the relative occurrence (cycle ratio) of stress amplitudes for the railway lines (a) Gothenburg-Skövde and (b) Skövde-Hallsberg. The dashed red lines show the stress amplitudes obtained from the telemetry system. The solid black lines show the stress amplitudes obtained from the probability distributions. The black vertical dashed lines and the black vertical dotted lines indicate the stress intervals in which $P_1$ and $P_2$ are respectively used to determine the statistical model of stress spectra. In between these areas, the statistical model is based on the probability distribution $P_{mid}$ (here represented by the central segment of the black solid curve).

acting on the axle, which does not vary for different routes. The occurrence of stress cycles drops significantly as the equivalent stress amplitudes increase, in particular for stress amplitudes larger than 60 MPa. However, this rapid decrease in the relative occurrence of equivalent stress amplitudes starts at lower amplitude levels for the route Skövde–Hallsberg, see Fig. 1(b), compared to the route Gothenburg–Skövde, see Fig. 1(a). As previously discussed, the two routes have similar maintenance statuses, so differences in track quality cannot significantly influence variations in stress spectra. These can be instead explained by looking at differences in track design (e.g., amounts of switches, crossings and narrow curves), which are summarised in Table 1.

| Railway line | Gothenburg–Skövde | Skövde–Hallsberg |
|---|---|---|
| Length of the line [km] | 143 | 109 |
| Number of switches and crossings (per km) | 0.59 | 0.39 |
| Number of curves (per km): | | |
| with curve radius lower than 1000 m | 0.43 | 0.04 |
| with curve radius lower than 700 m | 0.29 | 0 |

**Table 1:** Amount of switches, crossings and narrow curves per kilometre for the railway lines studied in Fig. 1. Data have been gathered from the BIS database of the Swedish Transport Administration

The comparisons in Table 1 show that, for the route Gothenburg–Skövde, the occurrence of switches and crossings is about 30% higher than for route Skövde–Hallsberg. Moreover, the route Gothenburg–Skövde is characterised by a significantly higher number of narrow curves (curves with radius lower than 1000 m are than ten times more frequent than for the route Skövde–Hallsberg). Two thirds of these curves have radii lower than 700 m for the route Gothenburg–Skövde, while no such sharp curves are present on the Skövde–Hallsberg route. The differences pointed out in this section can represent likely reasons for the increased frequency of higher stress amplitudes for the track section between Gothenburg and Skövde. Switches, crossings, curves and transitions curves, indeed, lead to discontinuities in the wheel–rail contact thus causing increased contact forces and axle stresses.

In order to be able to predict the stresses to which the axle is subjected while operating along a certain route, a procedure to obtain models of stress spectra based on statistical distributions has been developed. From the observation of the measured stress spectra (see Fig. 1 for some examples) it was determined that the most distinctive parts of the red dashed curves (the measured spectra) are the sections respectively characterised by a peak in the relative occurrence of stress cycles (this peak usually occurs at stress amplitudes between 35 MPa and 40 MPa) and the section where the frequency of measured stress levels declines (the sharp decline starts at stress amplitudes higher than 60 MPa). In between, there is a section characterised by a slower decline or by a plateau in the frequency of measured stress levels.

These two regions of the measured stress spectra have been modelled by fitting two normal distributions to the first and last parts of the curves plotted in dashed red line in Fig. 1. This procedure, which is based on the work performed in [4], has been applied to all the routes studied in this paper and the two distributions have been respectively named $P_1$ and $P_2$, see Fig. 1. It can be noticed that towards the centre of the stress spectra, these distributions do not longer follow the graph given by the measured stress amplitudes. In order to model the measured spectrum in a realistic way, as well as to connect the areas of the spectra described by the distributions $P_1$ and $P_2$, a third distribution named $P_{mid}$ was introduced. $P_1$ and $P_2$ have been truncated at the stress amplitude levels where the "cycle ratio" predicted by the normal distributions is 50% larger than the occurrence of the same stress amplitude level in the measured stress spectra, see the vertical dashed and dotted lines in Fig. 1. The points where distributions were truncated have been connected by a straight line in the semilogarithmic diagram and the distribution resulting from the area below that segment has been named $P_{mid}$.

## 3. Fatigue analyses

As discussed before, the telemetry system used in the present field test has been installed on a location of the axle where stress concentration effects are negligible. However, axles tend to crack more frequently in areas where stress concentrations are present, such as the T-notch, i.e. the fillet radius located below the wheel seat, see Refs [6] and [7]. The ratio between the in bending stress at the T-notch and that at the cross-section of the axle where the strain gauges are mounted was assessed to be in the order of 1.26. This was done in a static finite element analysis employing a three-dimensional model of the instrumented wheelset similar to the one used in Ref. [8]. A static stress concentration factor $k_t$ = 1.26 has then been adopted in this work.

To estimate the reduction in fatigue life of the axle due to varying operational conditions, the Wöhler curve (stress–cycles curve) for the T-notch of the instrumented axle was reduced according to Juvinall's method [9] according to the procedure described in Ref. [10]. The reduced fatigue limit at $10^6$ cycles $\sigma_{er}$ was thus obtained as:

$$\sigma_{er} = m_e m_t m_d m_s \sigma_u \tag{2}$$

where $\sigma_u$ = 600 MPa is the ultimate tensile stress (UTS) of the axle steel (EA1N), $m_e$ = 0.5 is the standard reduction factor for steels with $\sigma_u$ < 1400 MPa, $m_t$ = 0.9 accounts for the bending loading acting on the axle, $m_d$ = 0.8 is the size factor for the axle diameter. Lastly, $m_s$ (which depends on the material UTS) accounts for the axle surface condition. Moreover, the previously obtained Wöhler curve has been additionally reduced by the factor $k_f$ = 1.256 to account for the stress concentration at the T-notch. The factor $k_f$ is obtained from the stress intensity factor $k_t$ by using the approach from Peterson [11]. After all the reduction factors have been applied, the Wöhler curve consists of a straight line in a semilogarithmic stress-cycles chart connecting the stress amplitude at $10^3$ cycles $0.9 \cdot \sigma_u/k_f$ with the reduced fatigue limit at $10^6$ cycles $\sigma_{er}/k_f$.

Once the Wöhler curve has been reduced, different fatigue damage calculation algorithms can be adopted depending on the damage that stress cycles with an equivalent stress amplitude below $\sigma_{er}/k_f$ are supposed to generate. According to the first hypothesis (the least conservative one), stress cycles with amplitudes below this threshold do not cause any fatigue damage. The other two hypotheses assume that all cycles generate some fatigue damage: the most conservative one states that the fatigue damage caused by any stress cycle can be computed by simply prolonging the Wöhler curve without changing its slope. The other hypothesis, instead, assumes that damage of cycles with amplitudes below the reduced fatigue limit can be computed by prolonging the Wöhler with a reduced slope (only one third of the slope between $10^3$ and $10^6$ cycles). The damage

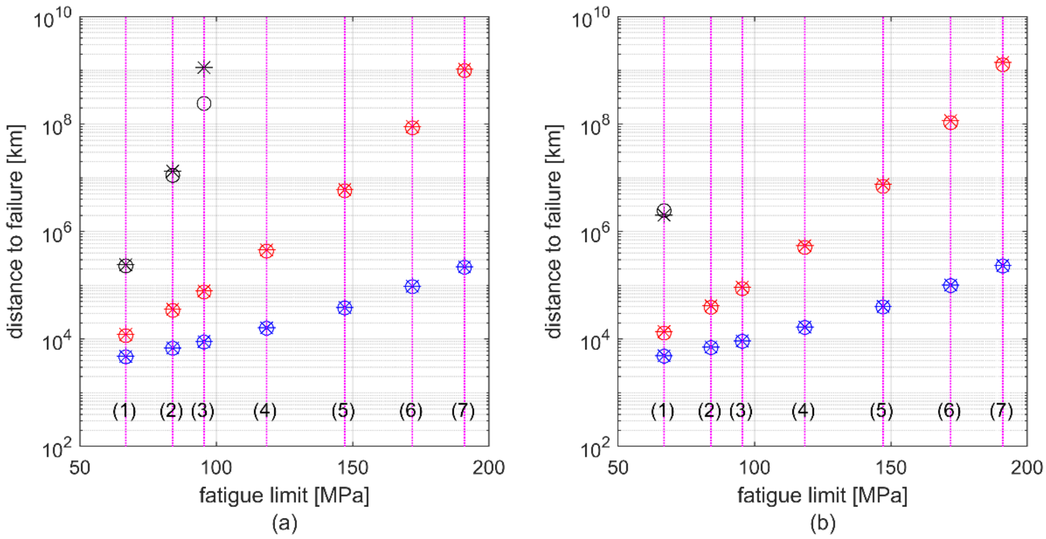


**Figure 2:** Estimated distance to failure for the instrumented axle for the stretches (a) Gothenburg–Skövde and (b) Skövde–Hallsberg. The fatigue lives marked with asterisks are obtained from the statistical models of stress spectra, while those marked with circles are obtained directly using spectra from the field test. Black markers indicate expected distances to failure if stress amplitudes below the fatigue limit are assumed not to cause any damage. The results in red and blue markers are based on the assumptions that the Wöhler curve is prolonged below the fatigue limit with respectively one third of the original slope and with unchanged slope. Fatigue limits correspond to axle surface conditions: (1) corroded in salt water, (2) as forged, (3) corroded in tap water, (4) hot-rolled, (5) machined, (6) fine-ground, (7) mirror polished.

accumulated after each stress cycle has been estimated using the damage accumulation procedure described by Palmgren [12].

Fatigue life analyses have been performed for the T-notch using as input both the stress spectra obtained from the measurements as well as those obtained from the fitted statistical distributions. In order to generate a stress history based on the statistical distributions, a Monte Carlo approach was used. Once the amount of cycles to be included in the whole stress history has been decided, cycles are allocated among the three distributions $P_1$, $P_{mid}$ and $P_2$ depending on their cumulative probability in the track section where the ride is to be simulated. Then, SWT stress amplitude values are generated according to the respective truncated probability density function. The fatigue damage caused by the resulting stress amplitude history can the be assessed. In order to account for a large variety of possible maintenance conditions, in particular relating to the axle surface conditions, different values for the surface roughness coefficient $m_s$ have been applied when reducing the Wöhler curve. The magnitude of $m_s$ affects the fatigue limits for $10^6$ cycles as shown by the dotted magenta vertical lines in Fig. 2.

No significant differences can be observed comparing fatigue lives computed from the measured stress spectra (plotted using circles) with those computed using the Monte Carlo procedure based on the statistical distributions (plotted using asterisks). This indicates that approximating stress spectra using statistical distributions leads to a low error when assessing the axle residual life. Moreover, Fig. 2 shows a strong dependency of the estimated axle fatigue on the axle surface conditions and on the damage accumulation algorithm adopted for stress cycles with amplitudes lower than the fatigue limit. It can also be noticed that no large differences are visible between of Fig. 2(a) and 2(b), in particular in the fatigue lives indicated by the red and blue markers (i.e., when low amplitude stress cycles contribute to the accumulation of fatigue damage). Although the stress spectra for the two railway stretches are different, the largest majority of stress cycles witnessed in service still fall within the probability distribution $P_1$. This distribution does not differ significantly between the two running cases. Its contributions in terms of stress cycles are relatively low in equivalent amplitudes, but they occur so frequently to generate the largest share of the total damage.

## 4. Conclusions

A method to obtain statistical models of bending stress spectra of railway axles has been presented. These models are based on truncated distributions fitted on spectra gathered during field tests. The residual fatigue life of the axle has been computed using stress histories from the field test or using the above-mentioned models as input. Results obtained using the two methods show a good agreement. Expected fatigue lives are however heavily dependent on the axle surface status and on the fatigue damage accumulation algorithm adopted.

As track properties in terms of presence of switches, crossings, curves, etc. can be linked to statistical stress amplitude distributions, these distributions can be used to discriminate between the quality of different track sections. The proposed method can contribute to the adoption of a condition-based maintenance approach by linking measured track conditions with the estimated residual fatigue lifetime of wheelset components.

## Acknowledgment

The current work is part of the activities within the Centre of Excellence CHARMEC (CHAlmers Railway MEChanics, www.chalmers.se/charmec). Parts of the study have been funded from the European Union's Horizon 2020 research and innovation programme in the project In2Track3 under grant agreement No. 101012456.

## References

[1] Grubisic V, Fischer G, “Procedure for reliable durability validation of train axles”, Materials Science & Engineering Technology, vol 37, 2006, pp 973–982

[2] Maglio M, Vernersson T, Nielsen J C O, Pieringer A, Söderström P, Regazzi D, Cervello S. “Railway wheel tread damage and axle bending stress – Instrumented wheelset measurements and numerical simulations”, International Journal of Rail Transportation, 2021, 23 pp

[3] Náhlík L, Pokorný P, Ševčík M, Fajkoš R, Matušek P, Hutař P, “Fatigue lifetime estimation of railway axles”, Engineering Failure Analysis, vol 73, 2017, pp 139–157

[4] Maglio M, Kabo E, Ekberg A, ”Railway wheelset fatigue life estimation based on field tests”, 2021, 25 pp

[5] Dowling NE, Kampe SL, Kral ML, “Fatigue of Materials: Introduction and Stress-Based Approach”, Chapter 9 from book “Mechanical Behavior of Materials”, 5th edition, Harlow (UK), Pearson Education Ltd, 2020, pp 375–449

[6] Lundén R, Vernersson T, Ekberg A, “Railway axle design: to be based on fatigue initiation or crack propagation?”, Proceedings of the Institution of Mechanical Engineers, Part F: Journal of Rail and Rapid Transit, vol 224, 2010, pp 445–453

[7] Madia M, Beretta S, Schödel M, Zerbst U, Luke M, Varfolomeev I, “Stress intensity factor solutions for cracks in railway axles”, Engineering Fracture Mechanics, vol 78, 2011, pp 764–792

[8] Maglio M, Pieringer A, Nielsen JCO, Vernersson T, “Wheel–rail impact loads and axle bending stress simulated for generic distributions and shapes of discrete wheel tread damage”, Journal of Sound and Vibration, vol 502, 2021, 19 pp

[9] Juvinall RC, Marshek KM, “Fundamentals of Machine Component Design”. 5th edition. Hoboken, New Jersey (USA), John Wiley, 2012

[10] Dowling NE, Kampe SL, Kral ML, “Stress-Based approach to Fatigue: Notched Members”, Chapter 10 in book “Mechanical Behavior of Materials”, 5th edition, Harlow (UK), Pearson Education Ltd, 2020, pp 450–516

[11] Peterson RE, “Stress Concentration Factors”, New York (USA), John Wiley, 1974, 336 pp

[12] Palmgren A, “Die Lebensdauer von Kugellagern” (Life span of Ball Bearings – in German), Zeltschrift des Vereines deutscher Ingenieure (Journal of the Association of German Engineers), vol 68, 1923, pp 339-341